

A model for focused ultrasound treatment of uterine fibroids

Colton Llyod
Aimee Raleigh
Ajay Sapre
Jessica Ungerleider

Presentation: November 22, 2013
Report: December 2, 2013

Table of Contents

Background.....	3
Problem Setup.....	4
Ultrasound and the Wave Equation.....	5
Heat Diffusion.....	7
Numerical Methods.....	10
Conclusions.....	13
References.....	16
Appendix A: MATLAB code.....	17

Background

Uterine fibroids also known as leiomyoma, leiomyomata, myoma, or fibromyoma are the most common benign tumor in women, affecting up to 60-77% of females by age 45 [1,2]. These tumors are benign and arise from smooth muscle cell proliferation. Most tumors are asymptomatic and can be left untreated, but significant, quality-of-life altering symptoms can occur. These vary depending on the size, location and number of fibroids and include pelvic pressure and pain, abnormal uterine bleeding, and reproductive dysfunction [1,2,3]. Fibroids can range from about 2cm to greater than 10cm in diameter [4]. Diagnosis is performed using ultrasound or MRI imaging modalities. In severe cases the most common form of treatment is hysterectomy, the surgical removal of the uterus, resulting in 200,000-315,000 cases per year [2,3]. Other treatment options include hormonal manipulation, laparoscopic surgery, and uterine artery embolization. As most women seek to preserve uterine function, there is a move to provide less invasive treatment with shorter recovery times. In recent years, magnetic resonance guided high-intensity focused ultrasound (MR g HIFUS) has been used as a noninvasive targeted treatment for fibroids.

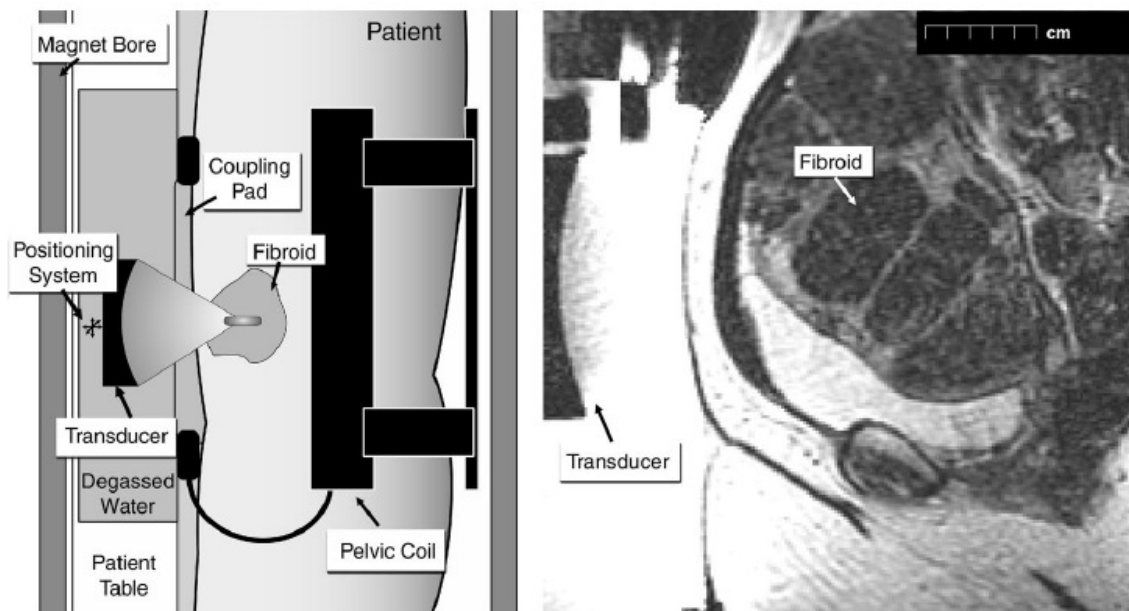


Figure 1. Ultrasound setup [5]

MR g HIFUS integrates MRI imaging and ultrasound ablation techniques into one system. MRI is used to determine the location of ablation and the subsequent temperature change. Coagulative necrosis is achieved by focusing ultrasound waves to the area of interest. This is done by using lenses, reflectors or phased arrays which control the attenuation of the beam. The focal point of this beam is a small volume that is much smaller than the volume of the tumor. Thus multiple sonications are required to achieve complete ablation where thermal energy is generated by acoustic absorption from the tissue. At the focal point, the temperature is increased relative to the power of the beam, which can heat tissue up to 65°C. Necrosis occurs only after surpassing a specific temperature/time threshold. For example, necrosis occurs when tissue is held at 50°C for 10 seconds, at 56°C for 1 second and at 60°C for 0.1 second [2]. Generally the ultrasound intensity is applied for 10-30 seconds and then turned off for about 90 seconds to prevent surrounding tissues from overheating. MRI thermal imaging is used to determine effective thermal dose. The total procedure takes about 2 hours for 60-90 ablations. MRgHIFUS is approved by the FDA for this use and is still under investigation for ablation of tumors of the breast, pancreas, prostate and liver [6].

Problem Setup

We wanted to model heat diffusion in a fibroid due to ultrasound ablation. This consists of two compartments: modeling of the ultrasound beam reaching the tumor and subsequent heat diffusion throughout the site of interest. The intensity of ultrasound would act as a source term in the diffusion model.

To model the thermal ablation of ultrasound, we chose a diseased state (uterine fibroids) in an area of the body that lacks any bony protrusions, so that we could assume scattering of the ultrasound beam was minimal. The uterus is mostly composed of smooth muscle, so we assumed that the fibroids were homogeneous and had a uniform diffusivity constant. We will assume that as the beam travels through the tissue to the tumor site, it is not attenuated, nor does it produce localized heating in the healthy endogenous tissue. Fibroids can assume a variety of shapes and relative sizes, but to simplify our problem we assumed that the fibroid would be spherical so that we could solve our diffusion equation in spherical coordinates. Moreover, we assumed symmetry in the fibroid so that the only space variable in our reduced equation was radial. Finally, we will simplify the tumor modeling by assuming it is avascular (and thus blood flow does not increase the localized heating at the site of ultrasound ablation). Although this is an incorrect assumption, the heat due to blood perfusion is much smaller than the clinically relevant temperature ranges of ultrasound ablation, so we feel that this assumption does not diminish the physiological relevance of the solution.

Because the size of the fibroid is relatively small in comparison to the body as a whole, we will assume that the body is infinite in size relatively. We will model several different iterations of ultrasound sonications (pulses). First, we will assume that the beam projection follows a cone profile as the energy produced by the total radiated power of all the transducers travels from the site of application through the bodily tissue. At the site of the tumor, the conical shape has converged into a tight distribution and thus all of the energy from the ultrasound is delivered to the fibroid in a very narrow range (excluding the healthy native tissue from the thermal ablation). In the very narrow range of high-energy ablation, we will assume that the ultrasound wave can be modeled as a Gaussian with a very narrow waist. In a second scenario, the Gaussian wave will be replaced with a Dirac Delta Impulse function in space.

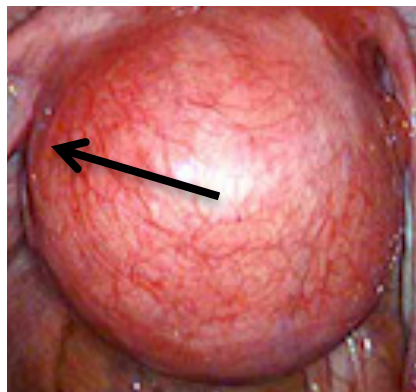


Figure 2. Fibroid in Spherical Coordinates

Table 1: Literature Values for Relevant Parameters

Parameter	Value	Units	Source
k (heat conductivity)	0.5	Watts/m/°C	10
Cp (specific heat of tissue)	3600	Watts*s/kg/°C	10
ρ (tissue density)	1000	kg/m ³	10

f_0 (ultrasound frequency)	1	MHz	8
α (tissue absorption component)	0.7	Db/cm @ 1 Hz	8
I_0 (ultrasound intensity)	1500	Watts/cm ²	7
w_0 (beam waist)	0.5	cm	8

Ultrasound and the Wave Equation

Although our main motivation in this problem is to analyze the heat diffusion in a uterine fibroid, we can expand upon the wave equation to derive a source term, which will represent the energy delivered by the sound wave once it reaches the region of ablation. This source term, as we will show in the following discussion, will consist of an overall intensity term as well as a Gaussian term.

We will be focusing on two main theories of wave propagation in the modeling of our ultrasound beam: Fourier Optics and the Huygens-Fresnel Principle. Both of these theories are centered on the assumption that the propagation of sound can be modeled as a linear phenomenon. Because there is independence in the spatial coordinates (for Cartesian, x, y and z), the solution to the wave equation is a superposition of each individual space component [11]. Because this wave propagation is linear, it can be approximated using a transfer function, specifically that of a Fourier Transform of the impulse response [11]. According to the theory presented by the two physicists Huygens and Fresnel, each wavefront consists of a collection of point sources. These point sources are each derived from spherical and increasing wave fronts that are modeled using a free space Green's function [12]. One slight discrepancy in Fourier Optics is that instead of representing each wave front as spherical and expanding, the sound waves are modeled as a superposition of plane waves which have no clear cut source of origin and instead arise as modes of the propagation medium [13]. Both of these theories serve as a starting point for our representation of traveling ultrasound pulses.

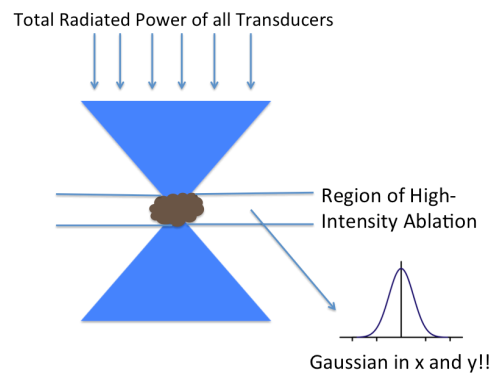


Figure 3. Simplified Representation of Ultrasound Wave Propagation

In our derivation of the wave equation, we began with a simple wave in time, represented as:

$$\left(\nabla^2 - \frac{1}{c^2} \frac{d^2}{dt^2}\right)U(\vec{r},t) = 0 \quad (1)$$

The Helmholtz equation is used in scenarios involving a source-free medium, and is derived from Maxwell's equation. Assuming we use a fixed frequency ultrasound then we can use the Helmholtz equation, which is only dependent on space:

$$\psi(\vec{r}) = a(\vec{r})e^{j\varphi(\vec{r})} \quad (2)$$

Where ψ represents a complex quantity involving a separate amplitude and phase

Substituting this back into the wave equation, we arrive at

$$(\nabla^2 + k^2)\psi(\vec{r}) = 0 \quad (3)$$

Where the wave number, $k = \frac{\omega}{c}$

Again, this solution is desirable because it is time-independent. Solving the “Fourier Optics” solution in Cartesian coordinates, the superposition of every individual component in x, y, and z gives:

$$\nabla^2 E_u + k^2 E_u = 0 \quad (4)$$

Solving this equation using a separation of variables technique:

$$E_u(x, y, z) = \int_{-\infty}^{\infty} \int_{-\infty}^{\infty} E_u(k_x, k_y) e^{j(kx_x + ky_y)} e^{+/- jz\sqrt{k^2 - kx^2 - ky^2}} dk_x dk_y \quad (5)$$

To model the Gaussian input, we assume that all of the ultrasound energy is being delivered to the tissue in the plane of the fibroid, which we will set to $z=0$. To model the Gaussian distribution in x and y:

$$f_0(x, y) = A_0 e^{[-B_0(x^2 + y^2)]} \quad (6)$$

Where A_0 represents the amplitude of the Gaussian and B_0 encompasses the beam width

We are ultimately interested in deriving a source term from the ultrasound wave propagation that will be input into the temperature diffusion equation to represent the energy delivered by the technology. Thus, we wish to square the amplitude (the A_0 term) and multiply this value by a Gaussian function. The complex equations for $A(z)$ and $w(z)$ (the beam “waist”) are as follows:

$$A(z) = A_0 \left(1 + j \frac{2B_0 z}{k}\right)^{-1} = A_0 \left(1 + j \frac{z}{z_0}\right)^{-1} = \frac{A_0}{\sqrt{1 + (z/z_0)^2}} \angle -\tan^{-1}(z/z_0) \quad (7)$$

$$w(z)^2 = w_0^2 \left[1 + \left(\frac{z}{z_0}\right)^2\right] \quad (8)$$

As the z coordinate moves away from the plane of ablation ($z=0$), the waist increases and thus the delivery of energy is represented by a Gaussian with a wider distribution, and thus a much lower energy. Simplifying to find the intensity term:

(9)

Where $I_0 = A_0^2$

Note that the β term is a lumped grouping of many constants. In fact,

$$\beta = \frac{2\alpha f * I_0}{C_p \rho} \quad (10)$$

With the literature values for these constants listed in Table 1

Overall intensity values in actual treatment regimens range from 1000-25,000 Watts/cm², but in many studies of uterine fibroid ablation is ~5000 W/cm² [7,8]. The value we chose to represent our ultrasound source term was 1500 W/cm² (see Table 1).

Heat Diffusion

In order to properly ablate the fibroid, the localized temperature must be raised to 50-80°C for short pulses of time. This increase in temperature results in protein denaturation, cell damage and necrosis with minimal damage to the surrounding native (and healthy) tissue. These sonications are usually in the range of 5 to 20 seconds [5]. We will begin with the standard temperature diffusion equation. As uterine fibroids are round in shape, we assumed the fibroid to be a homogenous sphere with no vascularization. This leads us to use a spherical coordinate system:

$$\frac{\partial T}{\partial t} = D \left(\frac{1}{r^2} \frac{\partial}{\partial r} \left(r^2 \frac{\partial T}{\partial r} \right) + \frac{1}{r^2 \sin \theta} \frac{\partial}{\partial \theta} \left(\sin \theta \frac{\partial T}{\partial \theta} \right) + \frac{1}{r^2 \sin^2 \theta} \frac{\partial}{\partial \psi} \left(\frac{\partial T}{\partial \psi} \right) \right) \quad (11)$$

Assuming diffusion is only the radial dimension and independent of θ and ψ then

$$\frac{\partial T}{\partial t} = D \left(\frac{1}{r^2} \frac{\partial}{\partial r} \left(r^2 \frac{\partial T}{\partial r} \right) \right) \quad (12)$$

As our ultrasound beam is a source of heat, we can add in a source term

$$\frac{\partial T}{\partial t} = D \left(\frac{1}{r^2} \frac{\partial}{\partial r} \left(r^2 \frac{\partial T}{\partial r} \right) \right) + Q(r)_{ext} \quad (13)$$

Where T is the temperature, D is the diffusivity, r is the radial dimension and Q is the ultrasound heat source (only dependent on r). From the derivation above (9)

$$Q(r)_{ext} = \beta e^{-\left(\frac{2r^2}{w_0^2}\right)} \quad (14)$$

Where w_0 is the beam width and $\beta = \frac{2\alpha f * I_0}{C_p \rho}$ (15)

Assuming the initial temperature of the tumor is

$$T(r, t = 0) = T_0 = T_{body} \quad (16)$$

The boundary condition at the center of the sphere

$$\frac{\partial T}{\partial r} (r = 0, t) = 0 \quad (17)$$

And boundary condition at the edge, $r=R$

$$T(r = R, t) = T_{body} \quad (18)$$

Solving the homogenous equation with separation of variables

$$T_H(r,t) = \Phi(r)G(t) \quad (19)$$

$$\frac{dG}{dt} \Phi(r) = \frac{D}{r^2} \frac{d}{dr} \left(r^2 \frac{d\Phi}{dr} \right) G(t) \quad (20)$$

$$\frac{1}{DG} \frac{dG}{dt} = \frac{1}{r^2 \Phi} \frac{d}{dr} \left(r^2 \frac{d\Phi}{dr} \right) = -\lambda \quad (21)$$

The time dependent solution is

$$\frac{1}{DG} \frac{dG}{dt} = -\lambda \quad (22)$$

$$\frac{1}{G} dG = -D\lambda dt$$

$$G(t) = e^{-D\lambda t}$$

$$(24)$$

And the radial dependent solution is

$$\frac{1}{r^2 \Phi} \frac{d}{dr} \left(r^2 \frac{d\Phi}{dr} \right) = -\lambda \quad (25)$$

$$\frac{d}{dr} \left(r^2 \frac{d\Phi}{dr} \right) = -r^2 \lambda \Phi \quad (26)$$

Solutions take the form of a linear combination of zero order spherical Bessel functions of the first kind:

$$\Phi(r) = \frac{A \cos \sqrt{\lambda} r}{r} + \frac{B \sin \sqrt{\lambda} r}{r} \quad (27)$$

Plugging in the homogenous boundary conditions we get

$$\Phi(r) = \frac{B \sin \sqrt{\lambda} r}{r} \quad (28)$$

$$\Phi(R) = \frac{B \sin \sqrt{\lambda} R}{R} = 0 \text{ since } B \neq 0 \text{ then } \sin \sqrt{\lambda} R = 0$$

thus $\lambda = \left(\frac{n\pi}{R}\right)^2$ for $n=0,1,2,3,4,\dots$

The homogenous solution is

$$T_H = \sum_{n=0}^{\infty} B_n \frac{\sin \sqrt{\lambda} r}{r} e^{-D\lambda t} \quad (29)$$

The eigenfunctions $\frac{1}{r} \sin\left(\frac{n\pi r}{R}\right)$ form a complete set of orthogonal eigenfunctions. Due to orthogonality, we must include a weighting factor of r^2 . Thus, we will multiply both sides of the above equation by the following:

$$r^2 \frac{1}{r} \sin\left(\frac{m\pi r}{R}\right) dr \quad (30)$$

Our coefficients B_n can then be calculated:

$$\sum_{n=0}^{\infty} \int_0^R B_n r^2 \frac{\sin\left(\frac{n\pi r}{R}\right)}{r} \frac{\sin\left(\frac{m\pi r}{R}\right)}{r} dr \quad (31)$$

$$B_n = \frac{\int_0^R r \sin\left(\frac{m\pi r}{R}\right) dr}{\int_0^R \sin^2\left(\frac{m\pi r}{R}\right) dr}$$

(32)

Reducing to:

$$B_n = \frac{2}{R} T(r,0) \int_0^R r \sin\left(\frac{n\pi}{R} r\right) 4\pi dr \quad (33)$$

We use the homogenous solution to represent the Green's function general form:

$$G(r,t;r_0,t_0) = \sum_{n=1}^{\infty} \frac{2}{R} \frac{1}{r_0} \frac{1}{r} \sin\left(\frac{n\pi}{R} r_0\right) \sin\left(\frac{n\pi}{R} r\right) e^{-D\left(\frac{n\pi}{R}\right)^2 (t-t_0)} \quad (34)$$

The full Greens solution accounts for the initial condition, the source term, the value boundary condition and the flux boundary condition

$$T(r,t) = \int_0^R T(r,0) G(r,t;r_0,0) dr_0 + \int_0^t \int_0^R Q_{ext} G(r,t;r_0,t_0) dr_0 dt_0 + \int_0^t T(R,t_0) \frac{d}{dr_0} G(r,t;R,t_0) dt_0 + \dots$$

$$\int_0^t \frac{d}{dr_0} T(0,t_0) G(r,t;0,t_0) dt_0 \quad (35)$$

Substituting the general form into the solution, we obtain

$$\begin{aligned}
T(r,t) &= \int_0^R \sum_{n=1}^{\infty} \frac{2}{R} T(r,0) \frac{1}{r_0} \frac{1}{r} \sin\left(\frac{n\pi}{R} r_0\right) \sin\left(\frac{n\pi}{R} r\right) e^{-D\left(\frac{n\pi}{R}\right)^2 t} 4\pi r_0^2 dr_0 + \dots \\
&\dots \int_0^t \int_0^R \sum_{n=1}^{\infty} \frac{2}{R} Q_{ext} \frac{1}{r_0} \frac{1}{r} \sin\left(\frac{n\pi}{R} r_0\right) \sin\left(\frac{n\pi}{R} r\right) e^{-D\left(\frac{n\pi}{R}\right)^2 (t-t_0)} 4\pi r_0^2 dr_0 dt_0 + \dots \\
&\dots \int_0^t \sum_{n=1}^{\infty} T(R,0) \frac{2}{R} \frac{1}{r} \sin\left(\frac{n\pi}{R} r\right) \frac{\partial}{\partial r_0} \frac{1}{r_0} \sin\left(\frac{n\pi}{R} r_0\right) e^{-D\left(\frac{n\pi}{R}\right)^2 (t-t_0)} dt_0
\end{aligned} \tag{36}$$

Since $\frac{\partial T}{\partial r}(r=0, t) = 0$, the flux term in the Greens function form is 0.

With the help of WolframAlpha, we obtain the full solution below:

$$\begin{aligned}
T(r,t) &= \frac{8}{n} T_0 \frac{R}{r} \sin\left(\frac{n\pi}{R} r\right) e^{-D\left(\frac{n\pi}{R}\right)^2 t} (-1)^n - \frac{2}{R} \frac{1}{r} \sin\left(\frac{n\pi}{R} r\right) \frac{1}{D\left(\frac{n\pi}{R}\right)^2} (1 - e^{-D\left(\frac{n\pi}{R}\right)^2 t}) \dots \\
&\dots 4\pi \frac{1}{16\sqrt{2}R} I_0 e^{-i\pi n} \omega_0^2 (\pi^{3/2} n \omega_0 e^{\frac{1}{8}\pi n (\frac{\pi n \omega_0^2}{R^2} + 8i)}) \operatorname{erfi}\left(\frac{4R^2 - i\pi n \omega_0^2}{2\sqrt{2}R\omega_0}\right) + \dots \\
&\dots \pi^{3/2} n \omega_0 e^{\frac{1}{8}\pi n (\frac{\pi n \omega_0^2}{R^2} + 8i)} \operatorname{erfi}\left(\frac{4R^2 + i\pi n \omega_0^2}{2\sqrt{2}R\omega_0}\right) + 2i\sqrt{2}(-1 + e^{2i\pi n}) \operatorname{Re} \left(\frac{2R^2}{\omega_0^2}\right) + \dots \\
&\frac{2}{R} T_0 \frac{1}{r} \frac{(-1)^n}{Dn\pi} \sin\left(\frac{n\pi}{R} r\right) [1 - e^{-D\left(\frac{n\pi}{R}\right)^2 t}]
\end{aligned} \tag{37}$$

To model the source term as an impulse (Dirac Delta function) instead of as a Gaussian distribution, the definition of the delta function in spherical coordinates was used:

$$\delta^3(r, \theta, \phi) = \frac{\delta(r)}{2\pi r^2} \tag{38}$$

Plugging this into the source term component of the general Green's function, we get:

$$\frac{8\pi}{R} \frac{\sin\left(\frac{n\pi}{R} r\right)}{r} \int_0^t e^{-D\left(\frac{n\pi}{R}\right)^2 (t-t_0)} dt_0 \int_0^R \frac{\delta(r_0)}{2\pi r_0^2} \frac{\sin\left(\frac{n\pi}{R} r_0\right)}{r_0} r_0^2 dr_0 \tag{39}$$

By solving each integral separately, we discover that the r integral reduces to just plugging in the value for r_0 into the $\sin(r_0)$ term. The sinc function at $r_0 = 0$ (assuming the delta source term occurs at the origin of the fibroid coordinate system) is just 1, so the integral reduces to $1/2\pi$. The entire source term component of the Green's function solution reduces to:

$$\frac{4R}{D(n\pi)^2} (1 - e^{-D\left(\frac{n\pi}{R}\right)^2 t}) \frac{\sin\left(\frac{n\pi}{R} r\right)}{r} \tag{40}$$

And the solution becomes the same as the full solution above (37), but with (40) in place of the source term solution (Figure 4).

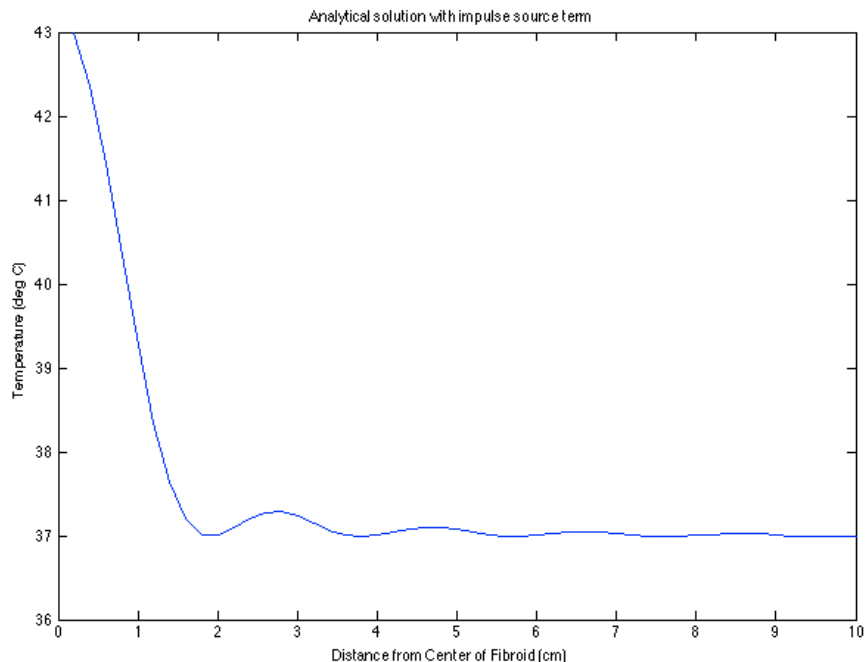


Figure 4: Analytical Solution with Impulse Source Term

Numerical Methods

The numerical solutions were found in MATLAB by concatenating two solutions found using MATLAB's PDEPE partial differential equation solver. The first PDEPE was solved using the $T(r,t=0)=37\text{ }^{\circ}\text{C}$ initial condition $T(r=R,t)=37\text{ }^{\circ}\text{C}$ boundary condition and the Gaussian Q_{ext} source term characterized above (Figure 5). The initial conditions for the second PDEPE solution were indexed from the first solution at $t=TPulse$ where $TPulse$ corresponds to the length of the sonication (Figure 6). These values were then exported to Excel where they were fit to a sixth order polynomial (Figure 7). The resulting fit curve was then used as the initial condition for the second PDEPE solution while maintaining the same boundary condition and setting the source term $Q_{\text{ext}}=0$.

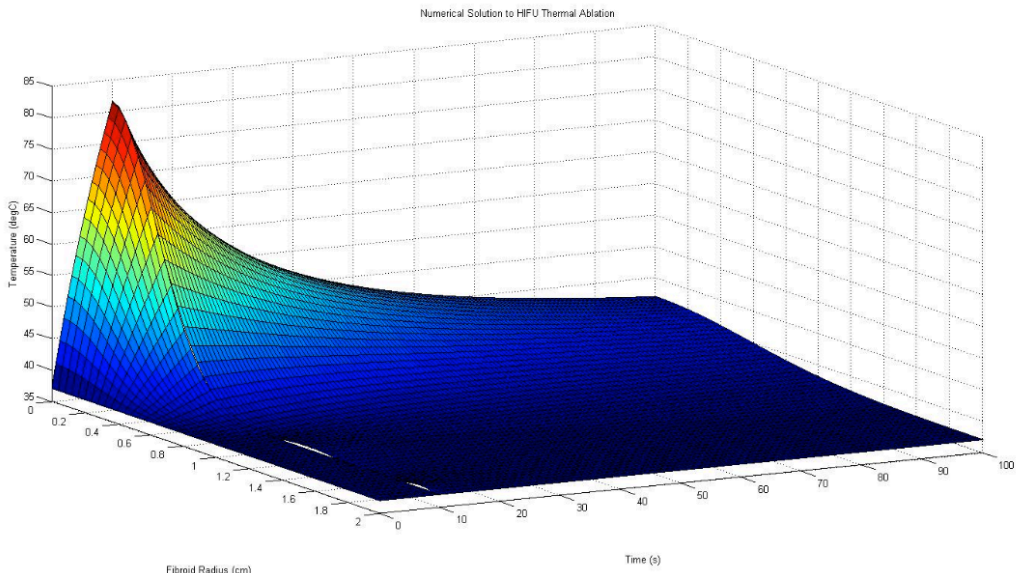


Figure 5. Gaussian Source Pulse and Subsequent Heating of Fibroid Tissue

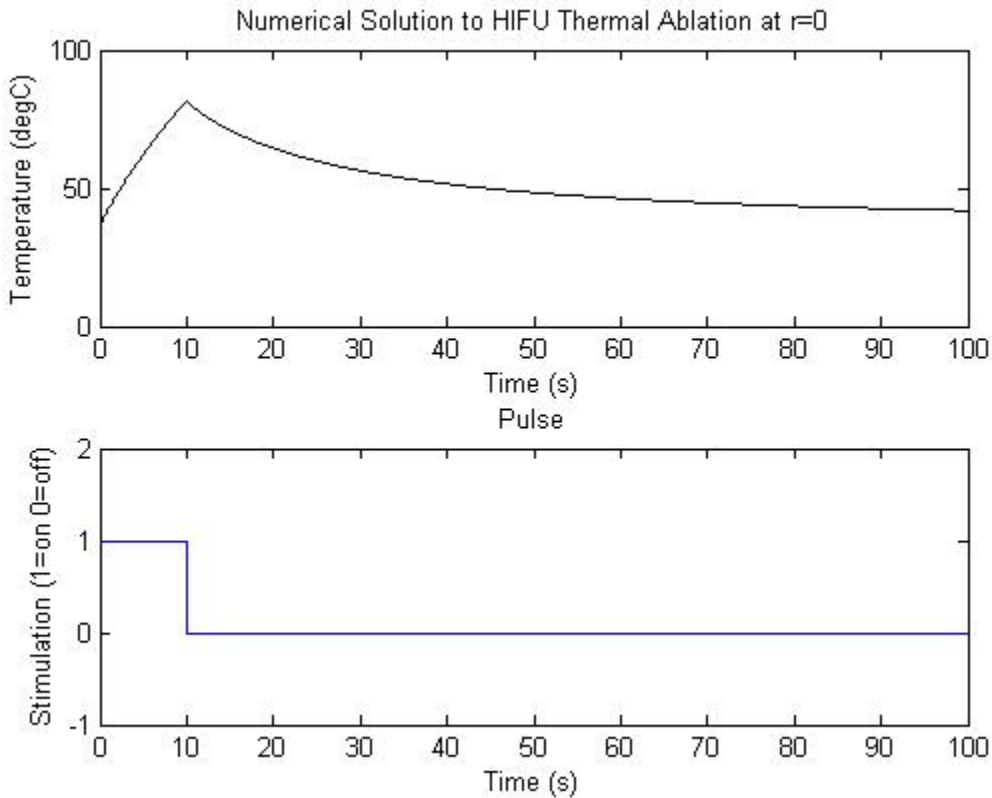


Figure 6: Numerical Solution at r=0 as Result of Single Pulse

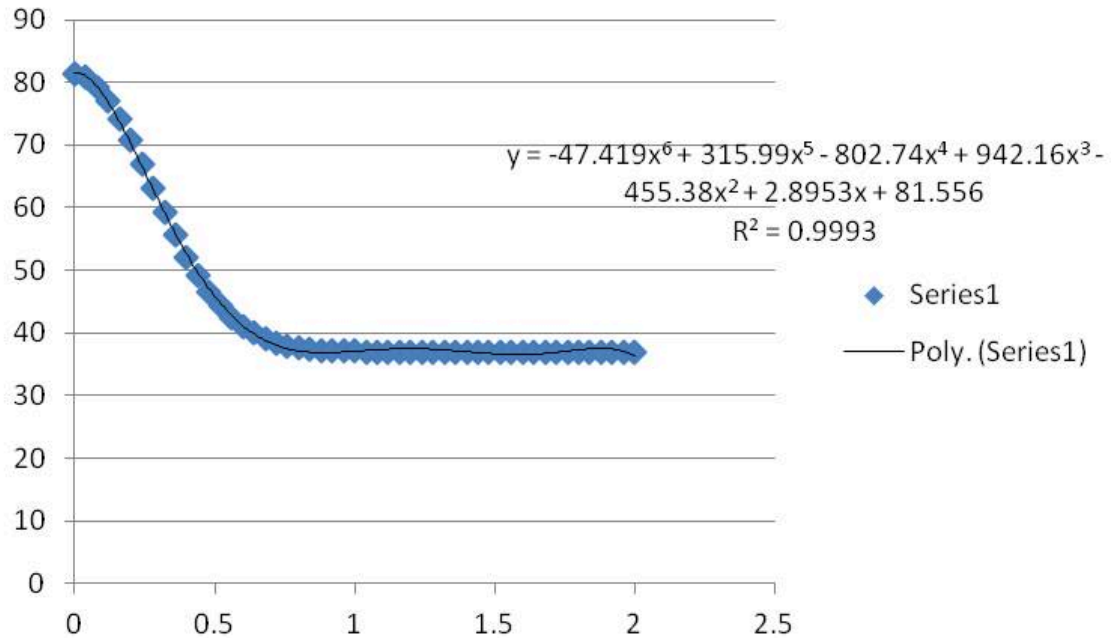


Figure 7. Excel Modeling of Ultrasound Pulse using a 6th Degree Polynomial

An additional two pulse model was solved in MATLAB by concatenating four PDEPE solutions (Figures 8&9). The same approach was taken for plotting the second pulse as the first, but the pulse time was shortened to 5 seconds in order to keep the temperatures obtained through the model within a relevant range. Additionally, the initial condition used for the beginning pulse was indexed from the second PDEPE solution at time equal to the start time of the second pulse.

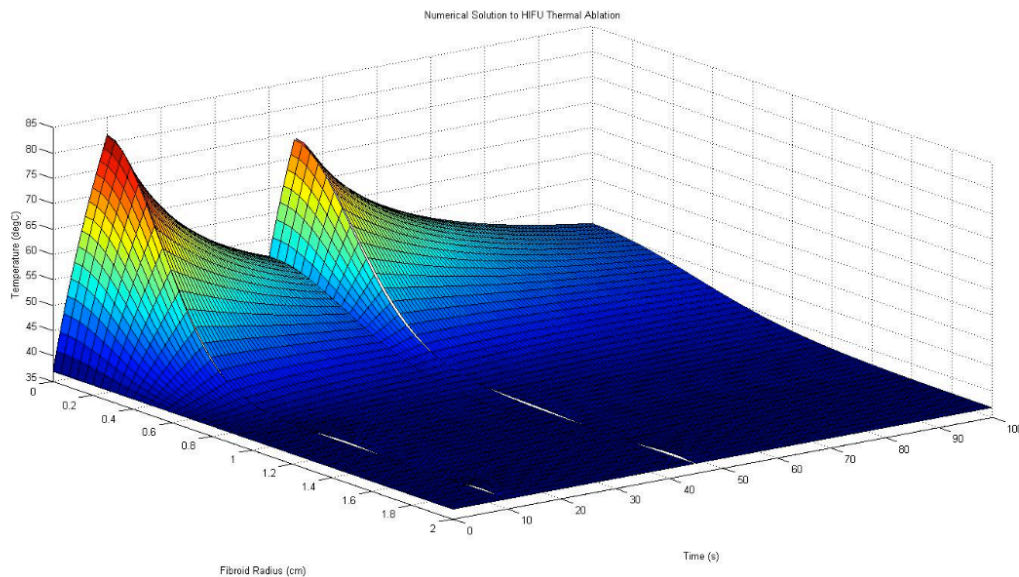


Figure 8. Gaussian Source Modeled as Two Distinct Pulses

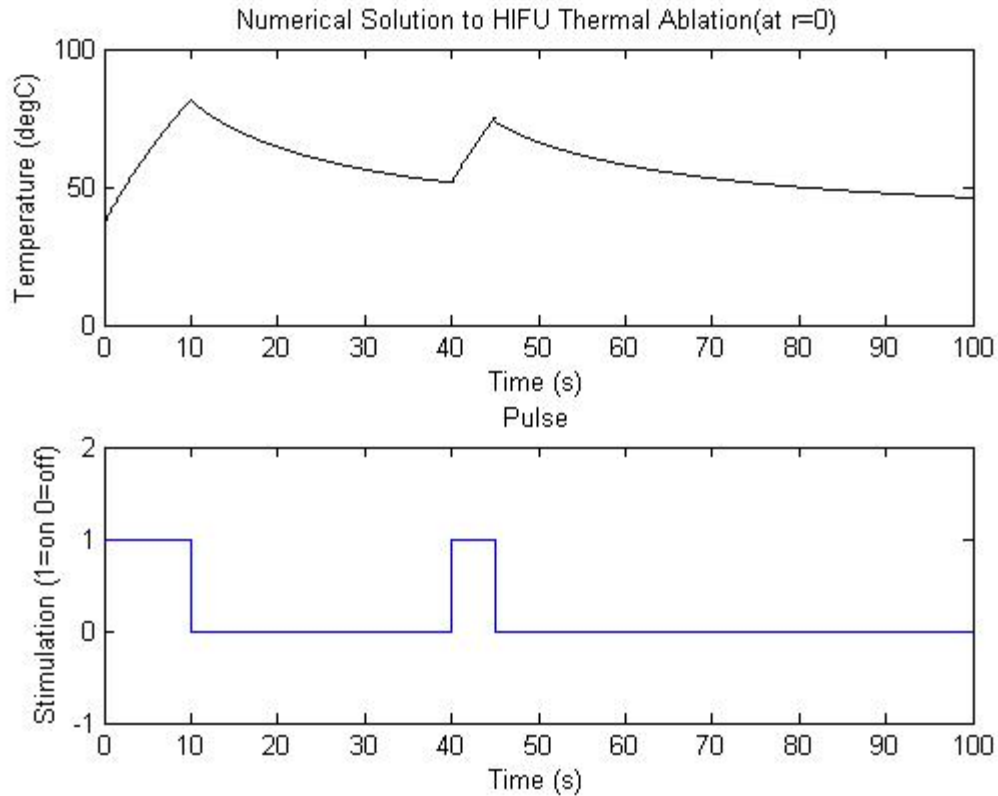


Figure 9: Numerical Solution at $r=0$ as a Result of Two Subsequent Pulses

Conclusions

Looking at the numerical solution using PDEPE (Figures 5, 6, 8, & 9), our MATLAB plots indicate a high level of ablation within the range of a typical fibroid (2-10 cm) and little heating of the tissue outside of this range. The temperature in all plots decreases rapidly to bodily levels (37°C) within 2 cm of the center of focus for the ablation. This result indicates a baseline level of safety for the technology, as one can assume low levels of heating and necrosis in native and healthy uterine tissue, an important point to consider for women who are still in their child-bearing years.

In addition, the numerical solution indicates potential for an even heat distribution throughout the fibroid. Especially focusing in on the dual ultrasound pulse (Figures 8&9), it is clear that multiple ultrasound pulses delivered in sequential order can improve the consistency of ablation throughout the tissue. This evidence may be used to support short pulses of ultrasound in treatment sessions to more evenly distribute the heat within the fibroid, while still maintaining safe temperatures in healthy tissue and keeping the maximum temperature within the fibroid at a reasonable value ($<80^{\circ}\text{C}$). These results suggest that our model may be used to suggest an optimization of ultrasound intensity and pulse timing to ensure desirable heating throughout the fibroid.

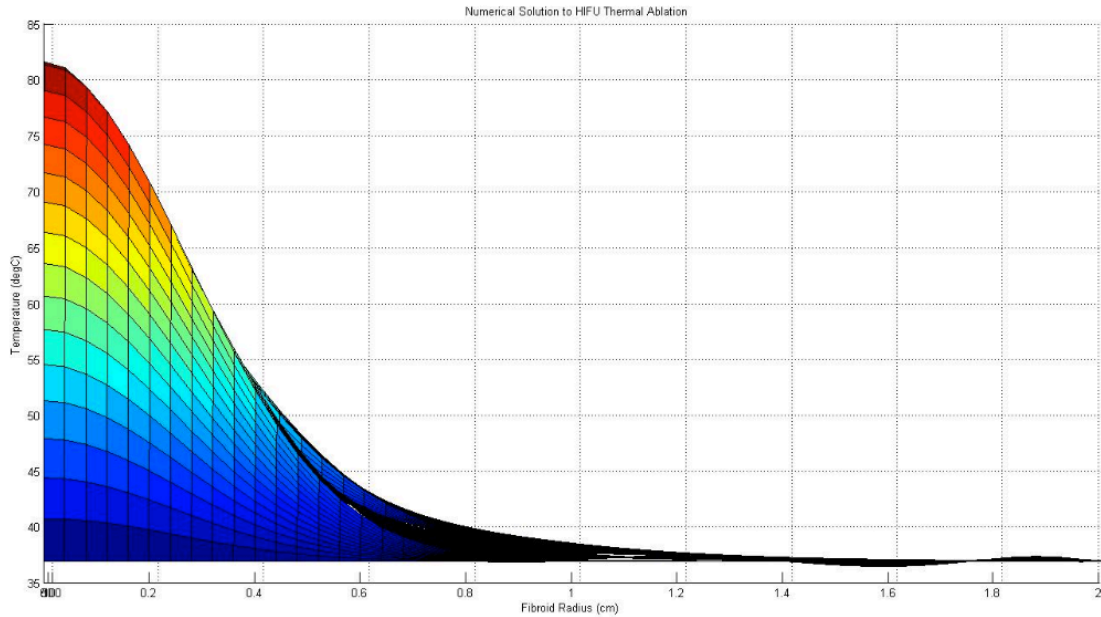


Figure 10. Effect of Additional Pulses on Thermal Ablation of Fibroid (profile view of Figure 7)

One of the most important conclusions drawn from our modeling work is that successful ablation was achieved with extremely low intensities compared to literature values. We chose an I_0 value of 1500 W/cm^2 , which was at the very bottom of the range suggested by published studies [7,8]. We experimented with varying levels for I_0 (data not shown), and found that the heat rose above clinically necessary temperatures [2]. This could mean that we oversimplified the physics of tissue absorption of ultrasound energy, meaning that the tissue would not absorb the energy and heat quite as efficiently. It is also possible that we did not effectively account for the extent which the intensity of the ultrasound beam will attenuate as propagates to the fibroid. It would be important to validate our model with clinical data of actual fibroid tumors to see if all of our assumptions hold. However, the fact that temperatures reached physiologically relevant ablation levels ($75\text{-}85^\circ\text{C}$) with only one or two pulses at relatively low intensities again indicates a safer technology that has minimal implications in the damage of endogenous tissues.

In future work, efforts should be made to model an entire treatment regimen, which can last between one and several hours and involve between sixty and ninety individual sonications of ultrasound [6]. Realistically, the current technology has precision to the millimeter, so it could be used to accurately ablate multiple locations within the tumor. A future model could also portray this realistic treatment scenario by having multiple ablations, not just at the origin/center of the fibroid. Based on our findings from multiple ultrasound pulses at the origin using PDEPE, we would expect multiple pulses at different locations to similarly distribute heat throughout the tissue more evenly. Furthermore, our model would be especially useful to ascertain whether these pulses throughout the tissue would do more damage to the healthy surrounding uterus.

Overall, this exercise was useful in measuring ultrasound wave propagation to uterine tissue and heat diffusion through that tissue. An especially valuable lesson learned from this project was that sometimes, numerical methods, while not as precise, can be a quicker and easier way to visualize the solution to the problem. Furthermore, we were even able to draw conclusions about the efficacy of ablation therapy from our PDEPE simulations.

References

- [1] Stewart, EA. Uterine fibroids. *The Lancet* 2001; 357: 293-298.
- [2] Roberts, A
- [3] Coakley *et al.*
- [4] Clare *et al.*
- [5] Tempany CM, Stewart EA, McDannold N, Quade BJ, Jolesz FA, Hynynen K. MR Imaging-guided Focused Ultrasound Surgery of Uterine Leiomyomas: A Feasibility Study. *Radiology* 2003; 226: 897-905.
- [6] Hesley GK, Gorny KR, Woodrum DA. MR-Guided Focused Ultrasound for the Treatment of Uterine Fibroids. *Cardiovascular Interventional Radiology* 2013; 36: 1077-1089.
- [7] Canney MS, Bailey MR, Crum LA. Acoustic characterization of high intensity focused ultrasound fields: A combined measurement and modeling approach. *The Journal of the Acoustical Society of America* 2008; 124: 2406-2420.
- [8] Curra FP, Mourad PD, Khokhlova VA, Cleveland RO, Crum LA. Numerical Simulations of Heating Patterns and Tissue Temperature Response due to High-Intensity Focused Ultrasound. *IEEE Transactions on Ultrasound* 2000; 47: 1077-1089
- [9] Thompson RB, Lopes EF. The effects of focusing and refraction of Gaussian ultrasonic beams. *Journal of Nondestructive Evaluation* 1984; 4: 107-123.
- [10] Gutierrez G. Study of the Bioheat Equation with a Spherical Heat Source for Local Magnetic Hyperthermia. *Mecánica Computacional* 2007; 26: 3562-3572.
- [11] Anderson ME, Trahey GE. A seminar on k-space applied to medical ultrasound. Duke University Department of Biomedical Engineering 2006. Available at: <http://dukemil.bme.duke.edu/Ultrasound/k-space/bme265.pdf>.
- [12] Born M, Wolf E. Historical Introduction. In: Born M, Wolf E, eds. *Principles of Optics: Electromagnetic Theory of Propagation, Interference and Diffraction of Light*. 7th ed. New York, New York: Cambridge University Press, 1999: xxv-xxxiii.
- [13] Goodman J. Linear Systems. In: Goodman J, ed. *Introduction to Fourier Optics*. 3rd ed. Greenwood Village, Colorado: Roberts & Co, 2005.

Appendix A: MATLAB Code

Numerical Solution

Matlab Code for Single Pulse

```
function BENG221Project_Numerical2
% initialize variables
clear all
close all
global R D T I0 w0 alph f0 cp p pulse IC1 xmesh
pulse=10; %duration of pulse

% following k cp p values from STUDY OF THE BIOHEAT EQUATION WITH A SPHERICAL
HEAT
% SOURCE FOR LOCAL MAGNETIC HYPERTHERMIA
k=.5; %Heat conductivity (W/m/degC)
cp=3600; %Specific Heat of tissue (W*s/kg/degC)
p=1000; %tissue (kg/m^3);

f0=1e6; %frequency of ultrasound used for treatment (Hz)
D = k/(p*cp)*100^2; %Thermal diffusivity (m^2/s)*100^2 cm^2/m^2=cm^2/s

w0 = .5; % waist at focal point
I0 = 15; %Peak intensity of ultrasound at x=focal point
R = 2; % outer radius of fibroid (cm)
T = 100; %end time
alph=.7; %tissue absorption coefficient (dB/cm at 1 MHz)
dx = R/50; % step size in x dimension
dt = T/150; % step size in t dimension
xmesh = 0:dx:R; % domain in x (cm)
tmesh = 0:dt:T; % domain in t (s)
T1=0:dt:pulse; % time array for duration of pulse
T2=pulse:dt:T; % array for time after pulse has ended

nx = length(xmesh); % number of points in x dimension
nt = length(tmesh); % number of points in t dimension

%Matlab pdepe
sol_pdepe = pdepe(2,@pdefunultra,@icultra,@bcultra,xmesh,T1);
IC1=sol_pdepe(length(T1),:);%index data to be used for initial condition
%for the second PDEPE solution
xlswrite('peak2',IC1) %export sol_pdepe data to excel
sol_pdepe2=pdepe(2,@pdefunultra2,@icultra2,@bcultra,xmesh,T2);

%surface plot of concatenation of all pdepe solutions
figure
```

```
surf(xmesh,T1,sol_pdepe)
hold on
surf(xmesh,T2,sol_pdepe2)
title('Numerical Solution to HIFU Thermal Ablation');
xlabel('Fibroid Radius (cm)');
ylabel('Time (s)');
zlabel('Temperature (degC)');

%plot numerical solution at r=0 for all time points
subplot(2,1,1)
plot(tmesh,0,T1, sol_pdepe(:,1,:), 'k',T2, sol_pdepe2(:,1,:), 'k')
title('Numerical Solution to HIFU Thermal Ablation at r=0');
xlabel('Time (s)');
ylabel('Temperature (degC)');
subplot(2,1,2)
step=ones(1,length(T1));
step2=zeros(1,length(T2));
steptotal=[step step2];

%plot time course for the single pulse
TT=length(tmesh);
plot(tmesh,steptotal(1:TT))
axis([0 100 -1 2])
title('Pulse');
ylabel('Stimulation (1=on 0=off)');
xlabel('Time (s)');

function [c, f, s] = pdefunultra(x, t, u, DuDx)
% PDE coefficients functions
global R D T I0 w0 alph f0 cp p
c = 1;
f = D*DuDx; % diffusion
s = 2*alph*f0*I0*exp(-(2*x^2/w0^2))/cp/p;

% -----
function u0 = icultra(x)
% Initial conditions function
global R D T E0 w0
u0 = 37;
% -----
function [pl, ql, pr, qr] = bcultra(xl, ul, xr, ur, t)
% Boundary conditions function
global R D T E0 w0
pl = 0; % inner boundary condition
ql = 0;
pr = ur-37;
qr = 0; % flux outer boundary condition
function [c, f, s] = pdefunultra2(x, t, u, DuDx)
```

```
global R D T I0 w0 alph f0 cp p pulse
c = 1;
f = D*DuDx;
s =0;%source term for pdepe2 after pulse=0
% -----
function u0 = icultra2(x)
% Initial conditions function
global R D T E0 w0
u0 = -47.419*x^6 + 315.99*x^5 - 802.74*x^4 + 942.16*x^3 - 455.38*x^2 +
2.8953*x + 81.556;
%u0 term derived from curve fitting of sol_pdepe(length(T1),:) in
%peak2.xls
% -----
function [pl, ql, pr, qr] = bcultra2(xl, ul, xr, ur, t)
% Boundary conditions function
global R D T E0 w0
pl = 0;
ql = 0;
pr = ur-37;% set right boundary condition to body temperature (37 deg C)
qr = 0;
```

Matlab Code for Two Pulses

```
function BENG221Project_Numerical2
% initialize variables
clear all
close all
global R D T I0 w0 alph f0 cp p pulse IC1 xmesh
pulse=10; %first pulse duration

pulsestart=40; % start time of second pulse
pulseend=45; % end time of second pulse

% following k cp p values from STUDY OF THE BIOHEAT EQUATION WITH A SPHERICAL
HEAT
% SOURCE FOR LOCAL MAGNETIC HYPERTHERMIA
k=.5; %Heat conductivity (W/m/degC)
cp=3600; %Specific Heat of tissue (W*s/kg/degC)
p=1000; %tissue (kg/m^3);

f0=1e6; %ultrasound frequency (Hz)
D = k/(p*cp)*100^2; %Thermal diffusivity (m^2/s)*100^2 cm^2/m^2=cm^2/s

w0 = .5; % waist at focal point
I0 = 15; %Intensity of ultrasound at x=focal point
R = 2; % outer radius of fibroid (cm)
T = 100; %final time (s)
alph=.7; %tissue absorption coefficient (dB/cm at 1 MHz)
dx = R/50; % step size in x dimension
dt = T/150; % step size in t dimension
xmesh = 0:dx:R; % domain in x (cm)
tmesh = 0:dt:T; % domain in t (s)
```

```
T1=0:dt:pulse; %time array for duration of first pulse
T2=pulse:dt:pulsestart; %time array for durating between end of first pulse
%and beginning of second pulse
T3=pulsestart:dt:pulseend; % time array for duration of second pulse
T4=pulseend:dt:T; %array for time after second pulse until end

nx = length(xmesh); % number of points in x dimension
nt = length(tmesh); % number of points in t dimension
%Matlab pdepe
sol_pdepe = pdepe(2,@pdefunultra,@icultra,@bcultra,xmesh,T1);
IC1=sol_pdepe(length(T1),:); %index sol_pdepe for time at the end of first
pulse
xlswrite('peak3',IC1) %export indexed data to excel

sol_pdepe2=pdepe(2,@pdefunultra2,@icultra2,@bcultra,xmesh,T2);
IC2=sol_pdepe2(length(T2),:); %index sol_pdepe2 at time=beginning of second
pulse
xlswrite('peak4',IC2)%export indexed data to excel

sol_pdepe3=pdepe(2,@pdefunultra3,@icultra3,@bcultra,xmesh,T3);
IC3=sol_pdepe3(length(T3),:); %index sol_pdepe3 at t=end of second pulse
xlswrite('peak5',IC3)%export indexed data to excel

sol_pdepe4=pdepe(2,@pdefunultra4,@icultra4,@bcultra,xmesh,T4);

%surface plot of concatination of all pdepe solutions
figure
surf(xmesh,T1,sol_pdepe)
hold all
surf(xmesh,T2,sol_pdepe2)
surf(xmesh,T3,sol_pdepe3)
surf(xmesh,T4,sol_pdepe4)
title('Numerical Solution to HIFU Thermal Ablation');
xlabel('Fibroid Radius (cm)');
ylabel('Time (s)');
zlabel('Temperature (degC)');

%plot numerical solution at r=0 for all time points
subplot(2,1,1)
plot(tmesh,0,T1, sol_pdepe(:,1,:), 'k',T2,
sol_pdepe2(:,1,:), 'k',T3,sol_pdepe3(:,1,:), 'k',T4,sol_pdepe4(:,1,:), 'k')
title('Numerical Solution to HIFU Thermal Ablation(at r=0)');
xlabel('Time (s)');
ylabel('Temperature (degC)');

%plot time course of all pulses
subplot(2,1,2)
step=ones(1,length(T1));
step2=zeros(1,length(T2));
steptotal=[step step2 ones(1,length(T3)) zeros(1,length(T4))]; %set up array
%of 0s for time not during pulse and 1s for time during pulse
```

```

TT=length(tmesh);
plot(tmesh,steptotal(1:TT))
axis([0 100 -1 2])
title('Pulse');
ylabel('Stimulation (1=on 0=off)');
xlabel('Time (s)');

function [c, f, s] = pdefunultra(x, t, u, DuDx)
% PDE coefficients functions
global R D T I0 w0 alph f0 cp p pulse
c = 1;
f = D*DuDx; % diffusion
s = 2*alph*f0*I0*exp(-(2*x^2/w0^2))/cp/p;

% -----
function u0 = icultra(x)
% Initial conditions function
global R D T E0 w0
u0 = 37;
% -----
function [pl, ql, pr, qr] = bcultra(xl, ul, xr, ur, t)
% Boundary conditions function
global R D T E0 w0
pl = 0; % inner boundary condition
ql = 0;
pr = ur-37;
qr = 0; % flux outer boundary condition
function [c, f, s] = pdefunultra2(x, t, u, DuDx)
% PDE coefficients functions
global R D T I0 w0 alph f0 cp p pulse
c = 1;
f = D*DuDx; % diffusion
s = 0; %source term for pdepe2 after pulse=0
% -----
function u0 = icultra2(x)
% Initial conditions function
global R D T E0 w0
u0 = -47.419*x^6 + 315.99*x^5 - 802.74*x^4 + 942.16*x^3 - 455.38*x^2 +
2.8953*x + 81.556;
%u0 term derived from curve fitting of sol_pdepe(length(T1),:) in
%peak3.xls
% -----
function [c, f, s] = pdefunultra3(x, t, u, DuDx)
% PDE coefficients functions
global R D T I0 w0 alph f0 cp p pulse
c = 1;
f = D*DuDx; % diffusion
s = 2*alph*f0*I0*exp(-(2*x^2/w0^2))/cp/p;
% -----
function u0 = icultra3(x)
% Initial conditions function
global R D T E0 w0

```

```

u0 = -3.3977*x^6 + 29.151*x^5 - 95.904*x^4 + 148.21*x^3 - 98.585*x^2 +
6.7067*x + 51.418;
%u0 term derived from curve fitting of sol_pdepe(length(T1),:) in
%peak4.xls
% -----
function [c, f, s] = pdefunultra4(x, t, u, DuDx)
% PDE coefficients functions
global R D T I0 w0 alph f0 cp p pulse
c = 1;
f = D*DuDx; % diffusion
s = 0; %source term for pdepe2 after pulse=0
% -----
function u0 = icultra4(x)
% Initial conditions function
global R D T E0 w0
u0 = -28.701*x^6 + 195*x^5 - 508.49*x^4 + 618.73*x^3 - 314.5*x^2 + 1.8867*x +
73.802;
%u0 term derived from curve fitting of sol_pdepe(length(T1),:) in
%peak5.xls

```

Matlab Code for Analytical Solution (Impulse Source)

```

k=.5;
cp=3600;
p=1000;
f0=1e6;
%D = k/(p*cp); %in um2/hr
D = 1e-3;
w = .01; % waist
I0 = 1500; %amplitude of insulin oscillation
R = 10; % outer radius of fibroid (um)
T = 10; %final time
T0=37;
alph=.7; %tissue absorption coefficient (dB/cm at 1 Hz)
dr = R/50; % step size in x dimension
dt = T/100; % step size in t dimension
rmesh = 0:dr:R; % domain in x (m)
tmesh = 0:dt:T; % domain in t (hr)
% nx = length(rmesh); % number of points in x dimension
% nt = length(tmesh); % number of points in t dimension
z = zeros(length(rmesh),length(tmesh));

    for j = 1:length(tmesh)
        for i = 1:length(rmesh)
            for n=1:10;

z(i,j) = z(i,j) + (4*R/(D*(n*pi)^2)).*(1-exp(-D*((n*pi/R)^2).*tmesh(j))).*...
                sin(n*pi.*rmesh(i)/R)./rmesh(i);

            end
            z(i,j) = z(i,j) + 37;
        end
    end

figure(1);
surf(tmesh',rmesh,z);

```

C.Lloyd
A.Raleigh

A.Sapre
J.Ungerleider

```
xlabel('Time (secs)');  
ylabel('Distance from Center of Fibroid (cm)');  
zlabel('Temperature (deg C)');  
figure(2);  
plot(rmesh,z(:,tmesh(length(tmesh))));  
xlabel('Distance from Center of Fibroid (cm)');  
ylabel('Temperature (deg C)');  
title('Analytical solution with impulse source term');
```